Mobility of grain boundary dislocations during the conservative untwisting of [001] twist boundaries

Siu-Wai Chan and V. S. Boyko
Henry Krumb School of Mines, Columbia University, New York, New York 10027
(Received 20 June 1995)

We modeled the mobility of grain boundary dislocations (GBD's) during the untwisting of the [001] twist boundaries. Instead of assuming two semi-infinite crystals in calculating the grain boundary energy (i.e., the Read-Shockley approach) and therefore the driving force for untwisting, we assume equally spaced GBD's moving in the (001) boundary plane with the dislocations closest to the surface being pulled out by the image force. Experimental results from crystallite rotation in fcc gold were used to investigate the mobility of the GBD's. Two types of GBD motion were tested: viscous and thermally activated. The observed motions of the GBD's during untwisting can be described only as thermally activated. The Hirth-Lothe approach, which involves a thermally activated process overcoming the Peierls barrier, was applied to describe the mobility of GBD's during untwisting into the $\Sigma 5$ cusp/minimum (Σ is the reciprocal of the density of the lattice sites in coincidence between two lattices at a misorientation) and the mobility of lattice dislocations $\{100\}\langle 110\rangle$ during untwisting into the $\Sigma 1$ cusp/minimum. The Peierls barrier for GBD motion confined to the glide plane of the boundary (001) is significantly higher than that for lattice dislocations glide on $\{111\}$ planes. From the untwisting rates, we estimate the energy barriers for GBD motions as 1.69 eV for $\Sigma 1$ and 1.84 eV for $\Sigma 5$ [001] twist boundaries. These results can explain the high yield stress and its sharp temperature dependence during plastic deformation of nanoparticle compacts of fcc metals. These results can also be used to estimate the largest size of crystallites that will rotate. [S0163-1829(96)06824-5]

I. INTRODUCTION

Grain boundary dislocations (GBD's) play an important role in the behavior of polycrystalline solids, particularly in superplasticity, grain boundary sliding, and migration. Geometrical properties of these GBD's have been investigated widely[1,2] and their elastic properties have been described, in a manner similar to that for lattice dislocations, within the framework of the theory of elasticity. The study of geometrical properties of lattice dislocations was followed by a period of experimental and theoretical investigations of their mobility, relating the acting forces and the velocities of these dislocations. Since then many studies have yielded data on lattice dislocation mobility in their normal glide planes, while few have dealt with either the mobility of lattice dislocations in other planes or the mobility of GBD's in the grain boundary planes. The situation concerning the mobility of grain boundary dislocations is different because of the difficulties of the observation of GBD's under controlled external loads. The usual experimental methods employed in studying the mobility of lattice dislocations simply do not apply for the GBD's.

Here we formulate a mathematical model that relates the GBD mobility observed by transmission electron microscopy (TEM) of crystallite rotations[3] with the forces acting on the GBD's. We also will consider the pure gliding of GBD's in a cooperative motion that causes the untwisting of pure twist boundaries. It is interesting to note that this approach can be applied not only to GBD's in high angle twist boundaries, but also to GBD's in low angle twist boundaries. When a crystallite of fcc structure untwists into the $\Sigma 1$ misorientation, this untwisting involves GBD's having the characteristics of pure screw lattice dislocations with Burgers vector $\mathbf{b}=(a/2)\langle 110\rangle$. Therefore, we can measure by this method the mobility of these lattice dislocations in (001) planes that are not the usual glide planes in the fcc crystal, a mobility difficult to measure by other methods.

II. PREVIOUS INVESTIGATION

In Chan and Balluffi's experiment[3,4] small gold crystallites (50–80 mm dia) were welded onto a (001) single-crystal gold thin film. After the welding, pure [001] twist boundaries existed in the welded neck regions, which could be observed directly by transmission electron microscopy at normal incidence. Upon annealing, the crystallites rotated about [001] into $\Sigma 1$ and $\Sigma 5$ misorientations (Σ is the reciprocal of the density of the lattice sites in coincidence between two lattices at a misorientation), indicating the existence of GBD-related cusps/minima on the boundary energy versus twist angle θ curve at these misorientations. The rotations occurred by the conservative motion of screw GBD's, which was observed directly by TEM in certain regions of θ. Original data of misorientation angle θ versus time t at 600 K for three crystallites rotating into $\Sigma 1$ are shown in Fig. 1.

The crystallite rotation experiment by Chan and Balluffi[3,4] was the first to observe the crystallite rotation in response to grain boundary structure and the corresponding GBD motions. In the untwisting of [001] twist boundaries,[3] their main purpose was to find out (a) if the crystallite rotation is sensitive to boundary energy variation with misorientation by observing the process particularly in real time and real space as compared to past observations with x-ray diffraction[5] where boundary dissociation and migration cannot be detected, (b) the GBD arrangements during untwisting, and (c) if any high angle Σ misorientations have deep enough energy

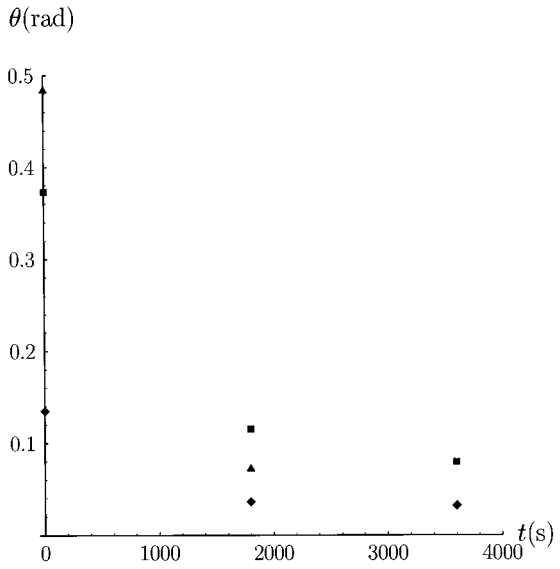

FIG. 1. The experimental data of angle-time dependence $[\theta(t)]$ of small particle rotation to $\Sigma 1$ misorientation: ▲, crystallite 1 (57 nm dia), ■, crystallite 2 (75 nm dia), ◆, crystallite 3 (55 nm dia).

minima to trap the untwisting crystallites. There was no attempt[3] to model the kinetics of the untwisting process although the evidence of a thermally activated process was mentioned.

This untwisting process merits a more detailed description. Crystallite rotations have been modeled by Shewmon[6] as a result of climb of GBD's for untilting and proposed by Pond and Smith[7] as a result of GBD's gliding for untwisting, though a correct formula for untwisting rate was not given.

A few years ago, Cahn[8] reexamined untwisting as a process initiated by the surface attraction of the nearest boundary dislocations. He assumed a simple geometry, half the space occupied by a semi-infinite vacuum and the other half by two crystals with an array of dislocations between them. He also showed that the untwisting rate slows down as the misorientation vanishes with no assumption about the retarding mechanism of the dislocation motions. This result is different from the rotation rate derived from a driving force based on the Read-Shockley equation of the boundary energy, where two semi-infinite crystals are assumed ignoring image forces associated with finite boundary areas. Such a simple approach is widespread in the literature. For example, both Li[9] and Erb and Gleiter[10] have taken the Read-Shockley equation and applied it to rotations of finite crystals. However, this approach gives an unrealistic infinite rotation rate as the spacings of GBD's become large.

It should be noticed that Chan and Balluffi,[3,4] conscious of the effect of the finite boundary area in their experiments, never applied the Read-Shockley equation in the modeling of untwisting but only in the untilting case when dislocation spacings were very small compared to the neck size of the boundary. Realizing the increasing influence of the image forces on the remaining GBD's, they did not apply the formulation in later stages when GBD spacings were large.

Later, King and Balasubramanian[11] used the Monte Carlo method to study untilting by a random variation of dislocation spacings. They found the rotation rate decreased with Monte Carlo time steps similar to Cahn's estimate.[8] They assumed a tilt boundary in a plate, but like Cahn[8] they did not take into account any of the diffusion mechanisms that are necessary for untilting. Neither of the two models[8,11] gives an exact kinetic mechanism or a rotation rate that can be compared directly to the measured rotation rates.

III. COMPUTATIONAL PROCEDURE

Here, we re-examine the situation with a detailed analysis of the untwisting rate based on the disappearance of the dislocations nearest to the boundary perimeter in the untwisting of [001] twist boundaries. Our modeling geometry consists of a twist boundary connecting the two surfaces of a plate. Inside this boundary, we have two parallel arrays of equally spaced right-hand screw dislocations with one array perpendicular to the other. We also assume no new surface created from the dislocation motions, which is consistent with the ball-on-plate experiment.[3] We have inevitably assumed that the rotation of GBD's by $(\Delta\theta/2)$ to accommodate the crystallite untwisting of $\Delta\theta$ is not an important kinetic step, a point which will be discussed later in this paper.

Let us consider the conservative untwisting of a low angle twist boundary due to the movement of screw dislocations towards the free surfaces and their escape from the boundary to the free surfaces. We will use the relationship between the velocity v as well as the acting force observed in experimental observation of dislocation mobility and will take into account that the process takes place in a bounded medium. In our model [Fig. 2(a)], we consider an infinite plate in vacuum or in air with a uniform thickness d. Separating the plate in two equal halves, the boundary runs from one free surface to the other. Dislocations in boundary are in two arrays: one is infinite in length and runs parallel to the surfaces; the other array runs perpendicular to these surfaces and is of length d. These two arrays practically do not interact with each other except to maintain mutual orthogonality so we can consider only one of these arrays with the assumption that the behavior of the other array will be the same. The second array is therefore neglected in the calculation of the untwisting rate. This geometry which forces the GBD's to retain their orientations is shown in Fig. 2(a), while a schematic representation of the experimental situation is shown in Fig. 2(b). We have studied a planar array of equally spaced screw GBD's, a configuration found experimentally. Figure 3 is a transmission electron micrograph showing the changes of GBD configuration during the final stage of untwisting of a $\Sigma 5$ boundary.

In the geometry of our boundary (Fig. 2) the dislocations nearest to the two surfaces escape from the crystal in the same way, so we can suppose that the behavior of the array is symmetric about the mid-plane of the plate. Here, we consider an array of screw dislocations in a plate with the geometry as shown in Fig. 2(a). The X axis is perpendicular to the free surfaces of the plate. The medium runs from $x=0$ to $x=d$, where d is the thickness of the plate. The Y axis is normal to the boundary on the ''left'' surface. The Z axis lies on the boundary and is parallel to the dislocation lines pointing out of the paper. If the coordinates of the first dislocation are $(x_0,0)$, and of another are $(x,0)$, then the interaction force

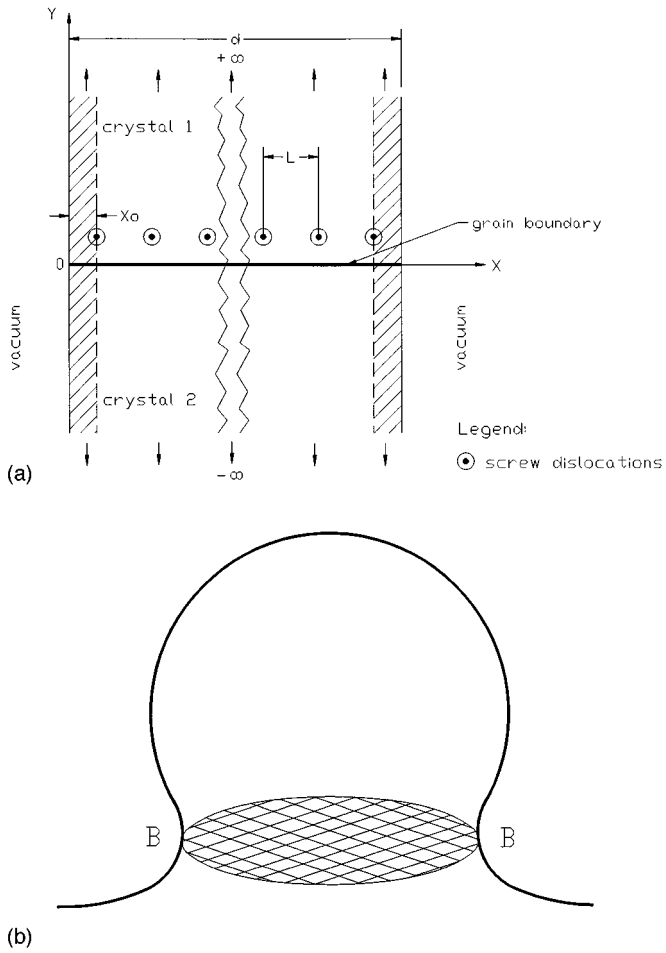

FIG. 2. The approach to the surface by an array of screw dislocation that causes the untwisting: (a) schematic representing the computational model (see text for details); (b) schematic representing the experimental situation. *BB* denotes the place of boundary location (the dislocation content of the boundary is shown schematically). [001] axis is perpendicular to the boundaries in both (a) and (b).

per unit length between these two screw dislocations can be written[12] as

$$F=\frac{\mu b^2}{4\pi d}\,\frac{\sin(\pi x/d)}{\cos(\pi x/d)-\cos(\pi x_0/d)}, \tag{1}$$

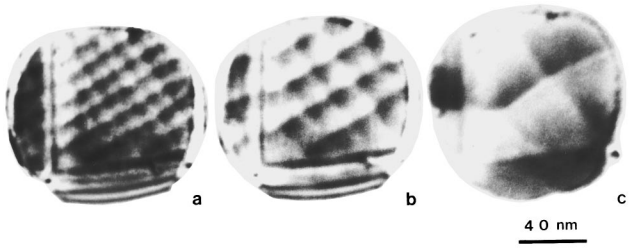

FIG. 3. Transmission electron micrographs showing grid of $\Sigma 5$ secondary screw GBD's in the neck region of a crystallite as it is rotated progressively from $\theta > 36.9°$ in (a) towards the $\Sigma 5$, $\theta = 36.9°$ in (b) and (c).

where b is the Burgers vector and μ is the shear modulus. Suppose that x_0 is the distance from the dislocation nearest to the ''left'' surface, and the dislocation spacing in the array equals L. As the first dislocation moves to the surface, x_0 decreases due to the image force and the interaction with all other dislocations in the array. We suppose, in accordance with experimental observations, that (a) these dislocations followed the first one while maintaining equal distances (L) between all dislocations in the array, and (b) all the m dislocations in the interval $x_0 \leqslant x \leqslant (d/2)$ move to the left surface and symmetrically all m dislocations at the interval $(d/2) \leqslant x \leqslant d$ move to the right surface. The collective force $F_{\rm int}$ acting on the first dislocation $(x_0,0)$ as the result of interaction with the other $(2m-1)$ dislocations is

$$F_{\rm int}=\frac{\mu b^2}{4\pi d}\,f_{\rm int}, \tag{2}$$

where $f_{\rm int}$, the dimensionless force, is given by

$$f_{\rm int}=\left(\sum_{k=1}^{m-1}\frac{\sin\{\pi[(x_0/d)+(k/2m)]\}}{\cos\{\pi(x_0/d)+(k/2m)]-\cos(\pi x_0/d)}+\sum_{k=0}^{m-1}\frac{\sin\{\pi[1-(x_0/d)-(k/2m)]\}}{\cos\{\pi[1-(x_0/d)-(k/2m)]\}-\cos(\pi x_0/d)}\right). \tag{3}$$

The stresses acting on a dislocation as the result of image forces can be obtained,[13] where the interaction of screw dislocations with two interfaces in a heterophase medium was considered. The heterophase medium was constructed as an isotropic plate between two elastic half-spaces. If we suppose that the elastic moduli of the two half-spaces go to zero, the image force $F_{\rm im}$ acting on a screw dislocation located at $(x,0)$ in a plate is[13]

$$F_{\rm im}=-\frac{\mu b^2}{2\pi}\int_0^\infty \frac{\sinh p(d-2x)}{\sinh pd}\,dp, \tag{4}$$

or after integration in a simpler expression,

$$f_{\rm im}=-\pi\,\tan\left[\frac{\pi}{2}\left(1-\frac{2x}{d}\right)\right],$$

$$F_{\rm im}=-\frac{\mu b^2}{4\pi d}\,f_{\rm im}, \tag{5}$$

where $f_{\rm im}$ is the dimensionless image force.

This expression describes the image force acting on a dislocation located at the point x in a plate. Indeed, when $x \to 0$ we obtain $F_{\rm im} \sim -(\mu b^2/4\pi x)$; if $x \to d$ we obtain $F_{\rm im} \sim (\mu b^2/4\pi)(1/d-x)$ and, lastly, when $x=(d/2)$ we obtain $F_{\rm im}=0$. Therefore, the resulting stress acting on the first dislocation from its own image as well as the stress of interaction with the other dislocations and their images in array can be expressed as

$$\sigma_{\rm sum}=\frac{\mu b}{4\pi d}\,f_{\rm sum}, \quad f_{\rm sum}=f_{\rm im}+f_{\rm int}. \tag{6}$$

The interval of time t_0 during which this dislocation escapes the solid medium can be written similar to Cahn's expression:[8]

$$t_0 = \int_{x_s}^{x_0} \frac{dx_0}{v(\sigma_{\text{sum}}, T)}, \tag{7}$$

where t_0 is the time for the first dislocation disappearance. It was shown by computer simulation[14] that a dislocation core approaching a free surface loses stability at a distance x_s from the surface equal to a few Burgers vectors (0.1–1 nm). Hence, the lower integration limit of (7) is x_s instead of zero.

Let us discuss the functional dependence of the dislocation gliding velocity v as a function of applied stress σ and temperature T: $v = v(\sigma, T)$ for GBD's. Nadgornyi[15] noted that from all experimental results the velocity of lattice dislocations can be expressed either in terms of an Arrhenius law in the thermally activated region or as $v = (b\sigma/B)$ in the viscous region, where $B = B(T)$ is the drag coefficient of dislocations. A twin boundary is a special high-angle boundary with a small Σ, so a twinning dislocation can be considered as an example of a GBD. The investigation of the mobility of twinning dislocations demonstrated (see Ref. 16 for details) that they basically have two modes of motion: continuous viscous flow and intermittent thermally activated motion. Based on this information, we consider the process of untwisting under two cases: (a) when the viscous motion of GBD's occurs, and (b) when the motion of GBD's is thermally activated. Under each case, the untwisting rate $(d\theta/dt)$ can be calculated through t_0 according to Eq. (7). Here $(d\theta/dt) \sim -(2b/dt_0)$, and $2\tan(\theta/2) = (b/L)$, where L is the dislocation spacing and θ is the angle of misorientation. The relationship has a minus sign because the angle decreases with time. The calculated rates were compared with the measured rotation rates to delineate between viscous flow or thermally activated GBD motion as well as to obtain data on the mobility of GBD's.

Naturally, our model cannot take into consideration all circumstances of the experiment. For example, we suppose that the dislocation array is located within a plate of two parallel smooth surfaces of the solid. In reality the region of surface that defines the perimeter of the boundary has a complicated configuration [see Fig. 2(b)]. An exact calculation of the elastic field of a dislocation near the surfaces cannot be carried out. We suppose also that all dislocations have infinite length and are parallel to each other. It is obvious that all the dislocations have a finite length. This outer surface of the neck region is not flat but of a cylindrical symmetry similar in geometry to the neck connecting a door knob to a door. As a result, the ends of the dislocation are bent near the surface so as to intersect the surface at right angles [see Fig. 2(b)]. Nevertheless, when the curved parts of the dislocation are very short compared to the straight segment of the dislocation, the present approach is valid. Figures 3(a), 3(b), and 3(c) show an extreme case when the untwisting approached a final stage when the end effect of dislocation can be important. Because of the large dislocation spacings in Figs. 3(a), 3(b) and 3(c), the GBD arrangements during untwisting are clearly shown. Therefore, present untwisting data for mobility calculation are taken when the straight segment of the dislocation is much longer than the curved parts.

IV. RESULTS AND DISCUSSIONS

We are now ready to compare the experimental and computational results. In the viscous case we obtain, by substituting $v = (b\sigma_{\text{sum}}/B)$ into Eq. (7),

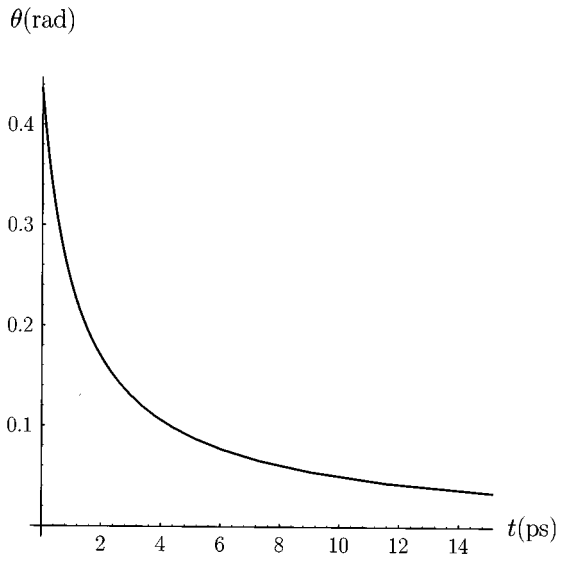

FIG. 4. Graph of the $\theta(t)$ for viscous motion of dislocations. Note that the time scale is in picoseconds.

$$t_0 = \frac{4\pi B d^2}{\mu b^2} \int_{(x_s/d)}^{(1/2m)} \frac{d\xi_0}{f_{\text{sum}}}, \quad \text{where } \xi_0 = \frac{x_0}{d}. \tag{8}$$

We calculate t_0 for the first pair of dislocations to escape, then for the second pair with m replaced by $m-1$, and so on. We can then compare the interval of time and the angle of rotation and obtain the dependence of θ on t, which will be compared with the experimental untwisting rates.

We first consider the untwisting of $\Sigma 1$ boundaries, with (001) as the boundary plane and $(a/2)\langle 110\rangle$ as the Burgers vectors (Fig. 1). We take $d \sim 55$ nm (the diameter of the neck in the experiment was 55–75 nm), $b \sim 0.3$ nm, $\mu \sim 3\times 10^{10}$ N/m^2, $B \sim 10^{-4}$ N s/m^2 (experimental values for B for fcc metals were given by Nadgornyi:[15] 57×10^{-6} N s/m^2 for Al and 20.3×10^{-6} N s/m^2 for Cu). The graph of $\theta(t)$ for these values of parameters is shown in Fig. 4. Comparing this graph with the experimental data shown in Fig. 1, we see that the time scale is off by ten orders of magnitude, which shows that expression (8) is completely unable to describe the experimental data. We conclude that viscous motion of screw GBD's was not operative in the experiments of Chan and Balluffi.[3]

Now we consider the case of thermally activated motion. The experimental observations of Chan and Balluffi[3] show that a thermal activation is required for untwisting of pure twist boundaries. Earlier observations[3] indicate that local ''barriers of some kind must be present which inhibit the otherwise glissile motion of the screw GBD's, but the detailed nature of these barriers is unknown.'' Nadgornyi[15] noticed that, in pure fcc metals, in the case of crystal lattice dislocations the resistance to their motion was extremely low on their usual slip plane, and, as a result, there is a widely held opinion that dislocation motion is viscous in most fcc metals. The motion of lattice dislocations in fcc metals for {111} glide planes will not experience Peierls barriers at the temperature range in question. When the same lattice dislo-

cations glide on {100} planes, it is expected that there is a larger Peierls force,[17] but, of course, there are few data bearing the point.

We cannot at present consider all circumstances defining the height of Peierls barrier for the observed GBD's. A consideration of the Peierls barrier for lattice dislocations according to Ref. 18 gives the expression:

$$\sigma_P \propto \frac{\mu}{1-\nu} \exp\left(-\frac{h}{b} \sqrt{\frac{2}{1-\nu}} \right),$$

where h is the planar spacing of the glide planes, and ν is the Poisson ratio. Therefore, the Peierls barrier depends both on the glide plane and the Burgers vector. A low angle [001] twist boundary must untwist on (001) and so the Peierls barrier will be a larger than that of a lattice dislocation with the same $\mathbf{b}=(a/2)\langle 110\rangle$ gliding on the wider spaced {111} planes. From this argument we can see that GBD's on high angle [001] twist boundaries ought to have a larger Peierls barrier. We must take into account also the fact that point defects can give additional contribution to the drag of GBD's, given that the density of point defects is usually greater at the grain boundaries than inside the crystal.

Such estimates compel us to consider the thermally activated motion of dislocations with high Peierls barriers by kink formation and propagation for dislocations gliding during untwisting $\Sigma 1$ and $\Sigma 5$. Following the approach described by Hirth and Lothe[17] we can write the expression for velocity of a dislocation in the form

$$v = v_0 \sigma_{\text{sum}} \exp\left(-\frac{E}{kT} \right). \tag{9}$$

Hirth and Lothe[17] considered two possibilities: (a) a situation of low stresses and strong obstacles for kinks propagation, i.e., a pair of kinks can propagate only on a limited segment of dislocation; and (b) a situation of high stresses and no obstacles, where there is no limitation on kinks propagation and kinks can propagate along dislocation until annihilation. Accordingly, in situation (a) $v_0=(b^3 s_v^2 \nu_D d/s_s^2 kT)$, where ν_D is the Debye frequency, s_s is the distance between the stable position of a kink along the dislocation line, and s_v is the distance between adjacent Peierls valleys; and $E=2F_k$, where F_k is the energy of kink formation (we suppose that limited segment of dislocation $\sim d$). In situation (b), correspondingly, $v_0=(2b^3 s_v^2 \nu_D/s_s kT)$ and $E=F_k$. When this approach[17] is used for consideration of lattice dislocation motion in covalent semiconductors with high Peierls barriers (see, for example, Refs. 19–21) it is supposed that a migrating kink feels a large potential variation (the secondary Peierls potential) along dislocation. Therefore the activation energy for kink migration E_m should also be taken into account. Then $E=2F_k+E_m$ in case (a) and $E=F_k+E_m$ in case (b). Since we are considering a situation of high stress and small volume, we will use case (b) for explaining our experimental data. Combining Eqs. (9) and (8) we obtain

$$t_0 = \left[v_0 \frac{\mu b}{4\pi d^2} \exp\left(-\frac{E}{kT} \right) \right]^{-1} \int_{(x_s/d)}^{(1/2m)} \frac{d\xi_0}{f_{\text{sum}}}. \tag{10}$$

The graph of the function $\theta(t)$ based on Eq. (10) for the case of the thermally activated motion of dislocations is shown on the Fig. 5. We take $d=55$ nm, $b=0.3$ nm, $\mu=3\times10^{10}$ N/m^2, $s_s \approx b$, $s_v \approx b$, $\nu_D \approx 10^{12}$ s^{-1}, $T=600$ K, $E \approx 2.71\times10^{-19}$ J (i.e., 1.69 eV).

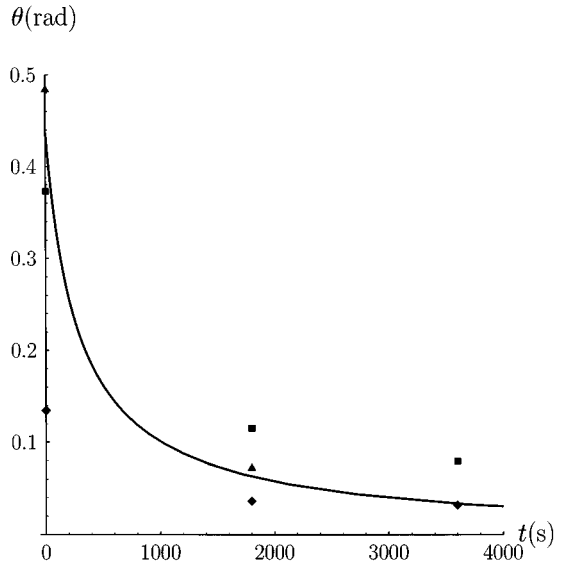

FIG. 5. Graph of the function $\theta(t)$ for thermally activated motion of {100}⟨110⟩ lattice dislocations. Superimposed is the experimental data from Fig. 1 for untwisting of $\Sigma 1$ [001] twist boundaries.

It is interesting to compare these data with that obtained by measuring the Bordoni peak with the internal friction method. This peak, as well known,[17] is attributable to double-kink formation along dislocations. The activation energy for the process in the case of gold has a value of 0.16 eV.[22] This activation energy is substantially smaller than our result, but in their case the lattice dislocations glide on {111} planes.

Now we consider the untwisting by GBD motion into the misorientation of $\Sigma 5$. Here, the Burgers vectors of GBD's are $(a/10)[310]$ and $(a/10)[130]$. The graph of the function $\theta(t)$ based on Eq. (10) for the case of the thermally activated motion of GBD's is shown in Fig. 6. We take $d=100$ nm, $b=0.1289$ nm, $\mu \approx 3\times10^{10}$ N/m^2, $s_s \approx 10b$, $s_v \approx 5b$, $T=723$ K, $\nu_D \approx 10^{12}$ s^{-1}, $E \approx 2.95\times10^{-19}$ J (1.84 eV). If we compare the computational and experimental results in Figs. 5 and 6, there is satisfactory agreement when we use the abovementioned values of parameters. We estimate that, in the $\Sigma 5$ case, the Peierls stress is a little greater than that in the case of $\Sigma 1$ where the screw GBD's have the same Burgers vector $\mathbf{b}=(a/2)\langle 110\rangle$ as lattice dislocations. We can suggest some explanation for this result. Computer simulation[23] has revealed structural units at the GBD core in fcc metals. Periodic entrance of these units in the core of moving GBD's would result in the appearance of additional ''grain boundary Peierls force.'' The higher Peierls stress reflects the more complicated rearrangement of atoms as the GBD's propagate in the $\Sigma 5$ boundary versus that in the $\Sigma 1$.

Thus, the GBD mobility based on experimental results shows that Peierls stresses are very high. Perhaps a high Peierls stress is not that uncommon, since lattice dislocations in semiconductors with diamond lattice have very large Peierls barrier.[15] For example, the experimental velocity for high-purity Si can be described[24] phenomenologically

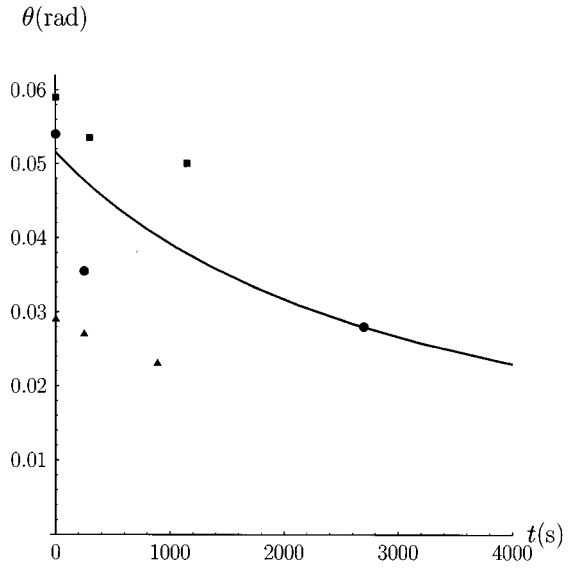

FIG. 6. Experimental data points and computational curve $\theta(t)$ calculated from the thermally activated model for the case of crystallite rotation into $\Sigma 5$ misorientation: ▲, sample 1 ($T=623$ K); ■, sample 2 ($T=673$ K); ●, sample 3 ($T=723$ K).

$$v = v_0 \sigma \exp\left(-\frac{\Delta H}{kT}\right), \tag{11}$$

where v_0 is constant, σ is external stress, and ΔH is activation enthalpy and equal to 2.35 eV for screw dislocations in silicon.[24] In the region of low stresses and low dislocation velocity, the authors of Ref. 24 can safely assume that ΔH is stress independent. The 2.35-eV value is close to our data with $E=1.84$ eV for GBD's on $\Sigma 5$ boundaries. Thus, we arrive at the conclusion that GBD's can have Peierls barriers as large as do lattice dislocations in diamond lattice. When we use expression (9) with reasonable values of corresponding parameters and calculate the above values of v_0, σ_{sum} as well as corresponding values of E, the calculated graphs $\theta(t)$ are close to experimental data (see Figs. 5 and 6, where these values are used).

At the same time we note that the present approach is valid for stresses normally much smaller than the elastic modulus (i.e., $\ll 0.01\mu$). The present stresses acting on dislocations are very high, and apparently the energy barrier could not be separated into individual kink energies and migration energy. In this case, calculation of kink formation and motion should include the elastic energy and the potential energy of the Peierls barrier.[17] Since the critical kink configuration is of the order of a few dislocation core radii, atomistic calculations are needed. Based upon the results of atomistic calculations of the Peierls barrier of twinning dislocations (see, for details Ref. 16) we can expect that the contours of Peierls energy relief for GBD's has a complicated shape with narrow and deep minima. Therefore, a consistent consideration of the situation is very difficult and beyond the scope of this article. We can expect that when high stress acts on a dislocation, the dislocation's velocity becomes a nonlinear function of stress. It would be reasonable to use an expression similar to (9) with a high power function dependence of stress with exponent as a phenomenological parameter. Generally, even in the stress range much smaller than the Peierls stress for the various kinds of semiconductors, the velocity of a lattice dislocations is generally expressed empirically similar to the following nonlinear function of the stress (see, for example, Refs. 19, 25, and 26):

$$v = v_0 \sigma_{\text{sum}}^n \exp\left(-\frac{E}{kT}\right), \tag{12}$$

where n is the stress exponent. The magnitude of n is measured to be between 1 and 2 (for Si, $n \approx 1$). In the range of high stresses magnitude of n should be increased. But there is no generally established view on this problem and it would bring complications (additional fitting parameter, for example), unwarranted at this stage of the work, when we want to show, principally, a possibility for applying our method to study GBD mobility. Here, we will show by a simple estimate that the motion of GBD's in our experiments is characterized by high energetic barriers. Let us rewrite expression (9) in the form

$$v = v_0 \Phi(\sigma_{\text{sum}}) \exp\left(-\frac{E}{kT}\right), \tag{13}$$

where $\Phi(\sigma_{\text{sum}})$ is a function of applied stress and could have the most common form. Then we can expect that $t_0 \propto \exp(E/kT)$ and $d\theta/dt \sim -(2b/dt_0) \propto -\exp(-E/kT)$. We will use our experimental data (see Fig. 6) when there are similar initial misorientations for different temperatures (723 and 673 K). Therefore we can suppose that the number of dislocations, and thus function's values of $\Phi(\sigma_{\text{sum}})$, are similar in both these cases. Using the correspondence experimental data we can estimate the initial angular velocities of the particles' rotation. Taking their ratio, we can estimate that the energy barrier for the GBD motion is on the order of eV. Therefore, we can conclude that the motion of GBD's in gold during the untwisting into $\Sigma 1$ and $\Sigma 5$ misorientations is thermally activated with high-energy barriers while the Hirth-Lothe approach[17] can be applied to describe the GBD motion. If we estimate F_k according to Ref. 17 as $(0.1-0.2)\mu b^2 s_v$, we can obtain from the above values of activation energies E's the formation energy of double kinks $F_k=0.51$–1.02 eV, the migration energy of the kinks $E_m=1.18$–0.67 eV for $\Sigma 1$, and, similarly, for $\Sigma 5$ screw GBD motion $F_k=0.2$–0.4 eV, $E_m=1.64$–1.44 eV. The kink migration energies in Si and Ge are both high and take an essential part of the apparent activation energy for the lattice dislocation motion.[27] Accordingly to earlier analysis,[28] the major contribution to the activation energy (1.3 eV) comes mainly from the kink migration energy for the glide of screw GBD's in a $\Sigma 9$ twist boundary in Si. It appears that a similar situation is realized in the two considered cases of GBD motion in gold.

An additional small detail: the rotation of the GBD's themselves by $(\Delta\theta/2)$ to accommodate the crystallite untwisting of $\Delta\theta$ probably proceeds against the same high Peierls stress that, overall, decreases the untwisting rate and gives rise to a higher apparent Peierls barrier that we have just calculated by assuming pure glide without GBD rotation. There is an additional circumstance in our experimental situation that can increase the energetic barrier for dislocation

motion. There are two sets of screw dislocations at right angles to each other. These two sets do not interact elastically, but they could be dragged by the contact interaction of dislocation cores. If there were an energy barrier for the translation of the overlapping cores of the two parallel dislocation arrays, the dislocations would not be straight but drag behind at each intersection. Since straight dislocations were observed, we can suppose that the translation of such overlapping cores has no appreciable energy barrier.

Finally, we estimate the thickness of the layer nearest to the surface that will not have dislocations, and the maximal size of crystallite that can be rotated. Near the surface, the layer free from dislocations can be determined from the condition $F_{\rm im}(x_0)>S_0b$, where S_0b is the force of dry or static friction. This force includes the Peierls force (for a given temperature) and the force needed to overcome barriers created by other lattice defects on the path of the considered dislocation (for details see Ref. 16). It is easy to show, using relationship (5), that inequality $F_{\rm im}\,(x_0)>S_0b$ is satisfied for all locations of dislocation near the free surface with $x_0<x_{0s}$, where

$$x_{0s}=\frac{d}{2}\left[1-\frac{2}{\pi}\tan^{-1}\left(\frac{4S_0d}{\mu b}\right)\right]. \tag{14}$$

x_0 is the thickness of the layer next to the surface that will not contain dislocations.

Now we consider the condition of crystallite rotation. The dislocation at the point x_1 in the array begins to move to the surface only if the condition

$$|(F_{\rm im}+F_{\rm int})|>|S_0b| \tag{15}$$

is satisfied. In order to obtain an estimate of the location of this dislocation we could use the simplified relationship for $F_{\rm im}$ and $F_{\rm int}$. We estimated the interaction between dislocations by considering the case of an infinite medium and assuming that the distribution of dislocations in the glide plane can be described by such a continuous function as the density of dislocations $\rho(x)$. In this case (see, for details, Ref. 17) $F_{\rm int}=(\mu b^2/2\pi)\int_0^d\rho(x)dx/(x_1-x)$. The singular integral in this expression is to be understood in the sense of principal value, i.e.,

$$F_{\rm int}=\frac{\mu b^2}{2\pi}\lim_{\Delta x\to 0}\left[\int_0^{x_1-\Delta x}\frac{\rho(x)dx}{x_1-x}+\int_{x_1+\Delta x}^{d}\frac{\rho(x)dx}{x_1-x}\right].$$

The distribution of dislocations in the glide plane is uniform: $\rho(x)=\rho_0=$const. Therefore we can estimate $F_{\rm int}\sim-(\mu b^2\rho_0/2\pi)\ln|(d-x_1)/x_1|$, $\rho_0\sim(1/L)$. We use a simplified expression for $F_{\rm im}$: $F_{\rm im}\sim-(\mu b^2/4\pi)[(1/x)-(1/d-x)]$. The location of the mentioned dislocation can be estimated from condition (15), in which we can use the above expressions for $F_{\rm int}$ and $F_{\rm im}$. Condition (15) can be written now in the form

$$\left|\frac{b(1-2\xi_1)}{2d\xi_1(1-\xi_1)}+\frac{b}{L}\ln\left|\frac{1-\xi_1}{\xi_1}\right|\right|>\left|\frac{2\pi S_0}{\mu}\right|, \tag{16}$$

where $\zeta_1=(x_1/d)$. The first term in (16) accounts for the image force; the second term accounts for the interaction between dislocations in the array. When the considered dislocation is nearest to a free surface (i.e., $x_1\lesssim x_0$), the particle would not be rotating at all. Therefore we can estimate the minimal size of this crystallite that would not rotate from (16) if we suppose that $\xi_1\lesssim(L/d)\sim(1/2m)$:

$$d\sim\frac{\mu b}{S_0}\,m\,\ln(2m). \tag{17}$$

Therefore, if we knew experimental data about maximal d for which particle can rotate we would estimate S_0 from condition (17) and vice versa. For example, if $(\mu/S_0)\sim10^2$, $m\sim10^2$ we obtain the reasonable value of $d\sim5\times10^4b$ for the minimal particle size that would not have visible rotation for some interval of time. Exact determination of this interval is needed in a more detailed consideration. When the temperature rises, the activated kink propagation mechanism of untwisting will be in effect, so the minimal d will increase.

Naturally, we conclude that the used values of thermally activated motion parameters of GBD's correspond reasonably well to the rotation rates recorded in the experiment. It is necessary to investigate them in a broader range of temperatures and angles to understand the escape of crystallites from $\Sigma13$ and $\Sigma17$ cusps/minima misorientations as observed.[3] But the present obtained results for $\Sigma1$ and $\Sigma5$ demonstrate that this thermally activated glide model agrees with the experiment and provides an opportunity to determine the type of obstacle hindering the GBD glide in the (001) plane.

Our results of high Peierls barriers for the glide of GBD's in grain boundary planes can explain the high yield stress observed in nanoparticle compacts of fcc metals.[29–31] In nanoparticle compacts, the motion of dislocations inside particles requires high shear stress concentrations. A significant number of boundaries are likely to be off the easy glide planes of {111} for GBD motions, which is one of the important deformation processes for nanoparticle compacts. This suggestion can explain the higher yield stress and the sharper temperature dependence of yield stress for nanoparticle compacts than for ordinary prepared metal samples, because deformation in nanoparticle compacts involves thermally activated GBD motion, which has an activation energy ~2 eV.[31]

V. CONCLUSIONS

An experimental-computational method is applied to study mobility of GBD's. It is shown that during the untwisting of twist boundaries, GBD gliding motion is not a viscous flow, but a thermally activated process, overcoming the Peierls barriers, i.e, lattice friction in the confined glide plane (001) of the boundary. The Hirth-Lothe approach for activated kink propagation can satisfactorily describe the motion of GBD's during untwisting into the $\Sigma5$ misorientation. The situation is the same in the case of lattice dislocations $\{100\}\langle110\rangle$ during the untwisting of the $\Sigma1$ grain boundaries. The barriers are estimated for the motion of these dislocations on the basis of experimental results. The possibility to estimate the largest size ($d\sim5\times10^4b$) of small particle that can be rotated by GBD motion is also shown.

ACKNOWLEDGMENTS

The authors would like to thank Dr. J. W. Cahn and Professor R. W. Balluffi, Professor D. N. Beshers, and Professor A. H. King for their comments and discussion, and Professor E. Nadgornyi for the discussion of mobility of lattice dislocations. S.-W.C. would like to acknowledge support from E. I. DuPont and Company and the National Science Foundation under Grant No. DMR-94-50464.

[1] R. W. Balluffi and G. B. Olson, Metall. Trans. A **16**, 529 (1985).
[2] R. C. Pond, in *Dislocations in Solids*, edited by F. R. N. Nabarro (North-Holland, Amsterdam, 1989), Vol. 8, Chap. 38, p. 4.
[3] S.-W. Chan and R. W. Balluffi, Acta Metall. **33**, 1113 (1985).
[4] S.-W. Chan and R. W. Balluffi, Acta Metall. **34**, 2191 (1986).
[5] G. Herrmann, H. Gleiter, and G. Bäro, Acta Metall. **25**, 467 (1977).
[6] P. G. Shewmon, *Recrystallization, Grain Growth and Textures* (American Society for Metals, Metals Park, OH, 1966), pp. 196–198.
[7] R. C. Pond and D. A. Smith, Scr. Metall. **11**, 77 (1977).
[8] J. W. Cahn, in *Sintering of Advanced Ceramics*, edited by C. A. Handwerker, J. E. Blandell, and W. Kaisser, Ceramic Transactions Vol. 7 (The American Ceramic Society, Westerville, OH, 1990).
[9] J. C. M. Li, Surf. Sci. **31**, 12 (1972).
[10] U. Erb and H. Gleiter, Scr. Metall. **13**, 61 (1979).
[11] A. H. King and L. Balasubramanian, Mater. Sci. Forum (to be published).
[12] V. S. Boiko, L. A. Pastur, and E. P. Fel'dman, Sov. Phys. Solid State **8**, 3284 (1967).
[13] V. S. Boyko, I. N. Sidorenko, E. P. Feldman, and V. M. Yurchenko, Phys. Met. Metall. **72**, 105 (1991).
[14] V. S. Boyko and V. A. Kirillov, Quest. Atom. Sci. Technol. Ser. Radiat. Damage Radiat. Technol. **28**, 83 (1983).
[15] E. Nadgornyi, in *Dislocation Dynamics and Mechanical Properties of Crystals*, edited by J. W. Christian, P. Haasen, and T. B. Massalski, Progress in Material Science Vol. 31 (Pergamon, Oxford, 1988).
[16] V. S. Boyko, R. I. Garber, and A. M. Kossevich, *Reversible Crystal Plasticity* (AIP, New York, 1994).
[17] J. P. Hirth and J. Lothe, *Theory of Dislocations* (Wiley Interscience, New York, 1982).
[18] A. H. Cottrell, *Dislocations and Plastic Flow in Crystals* (Clarendon, Oxford, 1953).
[19] H. Alexander, in *Dislocations in Solids*, edited by F. R. N. Nabarro (North-Holland, Amsterdam, 1986), Vol. 7, Chap. 35, p. 113.
[20] K. Maeda and Y. Yamashita, Phys. Status Solidi A **138**, 523 (1993).
[21] R. Hull and J. Bean, Phys. Status Solidi A **138**, 533 (1993).
[22] D. N. Beshers and R. J. Gottschall, in *Internal Friction and Ultrasonic Attenuation in Crystalline Solids*, edited by D. Lenz and K. Lücke (Springer-Verlag, New York, 1975), Vol. 2, p. 134.
[23] A. P. Sutton, D. A. Smith, and V. Vitek, J. Microsc. **116**, 97 (1979).
[24] M. Imai and K. Sumino, Philos. Mag. A **47**, 599 (1983).
[25] K. Sumino, in *Structure and Properties of Dislocations in Semiconductors*, edited by S. G. Roberts, D. B. Holt, and P. R. Wilshow, IOP Conf. Proc. No. 104 (Institute of Physics and Physical Society, Bristol, England, 1989).
[26] H. Siethoff, Phys. Status Solidi A **138**, 591 (1993).
[27] B. Farber *et al.*, Phys. Status Solidi A **138**, 557 (1993).
[28] H. A. Benhorma, A. Jacques, A. George, and X. Baillin, Phys. Status Solidi A **131**, 539 (1992).
[29] G. W. Nieman, J. R. Weertman, and R. W. Siegel, Scr. Metall. **23**, 2013 (1989).
[30] G. W. Nieman, J. R. Weertman, and R. W. Siegel, Scr. Metall. Mater. **24**, 145 (1990).
[31] G. W. Nieman, J. R. Weertman, and R. W. Siegel, J. Mater. Res. **6**, 1012 (1991).